RESEARCH
www.commprac.com
ISSN 1462 2815

ULTRA-STRUCTURE ANALYSIS OF APOPTOSIS INDUCED BY SILVER NANOPARTICLES IN BREAST CANCER MCF 7 VIA INDEPENDENT mTOR- PATHWAY

Fawziah A. AL-Salmi *

Department of Biology, Faculty of Sciences, Taif University, Taif, Saudi Arabia.
*Corresponding Author Email: f.alsalmi@tu.edu.sa

DOI: 10.5281/zenodo.10029517

Abstract

The aim of this study is to provide evidence of the ability of silver nanoparticles to induce autophagy-associated apoptosis. In this report, silver nanoparticles exhibited time-dependent cytotoxicity in breast cancer cells. Multiple assays verified that the activity of silver nanoparticles to induce autophagy blocked the autophagic flux at 50µg/ml. Furthermore, Ag-NPs impaired lysosomal function by damaging lysosomal ultrastructures. The results revealed that silver nanoparticles activated apoptosis at 39.2% and arrested the cell cycle at S phase due to an increase in the percentage of cells at S phase of 10 percent as compared with non-treated cells. The rt-Pcr results showed downregulation of LC3, AKT, and mTOR. The LC3 gene is an autophagic gene that regulates the autophagy process. The immunohistochemistry showed weaker AKT, while Caspase 3 showed strong immunochemistry staining. Transmission electron microscopy showed autophagosomes that are considered the benchmark for autophagy studies; the number of double-membrane autophagosomes and single-membrane autolysosomes was obviously observed in Ag-NP-treated MCF-7. Finally, these results indicate that the cytotoxicity of Ag-NPs may involve the autophagic pathway in MCF-7 cells.

Keywords: m-TOR, AKT, LC3, Caspase 3, Silver Nanoparticles, Autophagy, Apoptosis, Breast Cancer, Ultra-Structure Analysis

INTRODUCTION

Globally, breast cancer is a massive malignancy leading to death. Cancer of the breast is caused by the growth of the cells that has a special feature of being uncontrolled in nature [1]. The breast cancer occurrence is either being in breast lobular, in this case its name is going to be lobular carcinoma in situ or in the ducts and it is called ductal carcinoma in situ [2]. Furthermore, breast cancer is divided into two classes: non-invasive breast cancer, in which breast cancer cells do not migrate. While the breast cancer cells that transfer into the surrounding cells are called non-invasive breast cancer [3]. Breast cancer is considered an aggressive disease and should be early diagnosed, with therapies leading to the best prognosis [4].

The most common effective drugs that are recommended for advanced stages of breast cancer are sorafenib (SOR) and lenvatinib, which belong to the multikinase inhibitors [3]. The PI3K-Akt-mTOR signaling pathway has effects in the tumor microenvironment, such as interactions with immune cells and activation of the inflammatory response [5–6]. Akt, a serine/threonine kinase also known as protein kinase B, has a down-regulated influence on the PI3K/Akt/mTOR cascade [7] and the activity of Akt as a result of the suppression of apoptosis. The mammalian target of rapamycin (mTOR) is another member of the PI3K-related kinase family. mTOR, including two protein complexes: mTORC1 and mTORC2 [8]. mTORC1 has a central role in cell growth and metabolism, while mTORC2 is closely related to cell proliferation and mechanisms of survival [9].

The phosphoinositide 3-kinase (PI3K)/serine-threonine protein kinase (AKT)/mTOR signal pathway is highly activated in many cancer cells [10], and the inhibition of the PI3K/AKT/mTOR signal pathway can inhibit the growth, invasion, and metastasis of various tumors such as colon cancer [11] and breast cancer [12]. The ability of the PI3K/AKT pathway to activate AKT, which controls and regulates the cell cycle, apoptosis, metastasis, and angiogenesis [13], is its distinguishing feature. As a result, many researchers are focusing on targeting the PI3K/Akt pathway in anti-cancer agents [14]. The PI3K/AKT/mTOR signal pathway regulates autophagy [15], because mTOR is the target molecule of the cell autophagy pathway [16]. The mechanism of phosphorylate autophagy is related to protein 13 (ATG13), which prevents binding to ATG1, leading to the formation of the autophagosome [17].

Globally, there has been an exponential growth in the application of nanomedicine in the last twenty years, which has led to great advances in the fabrication of new nanomaterials and their applications [18–19]. The novel nanomaterials have contributed to many innovations during the present decade [20]. For example, silver nanoparticles have multiple applications in biomedical fields such as cancer diagnosis and therapy, antibacterial [21], antiviral [22], and tissue engineering [23]. In this work, silver nanoparticles was prepared using *Aspergillus niger* as a novel approach of synthesis nanomaterials with green methods, then prepared silver nanoparticles on the breast cancer cell by cell viability assay, apoptosis assay and study the effect of the Ag-NPs on autophagy gene LC3, Akt and mTOR and apoptosis using the RT-PCR, Immunohistochemistry and observed the morphemically changed in the cell during treatment with silver nanoparticles using transmission electron microscopy.

MATERIAL AND METHODS

Green synthesis of silver nanoparticles

In this study, silver nanoparticles (Ag-NPs) were synthesized using a biological approach using microorganisms instead of chemical methods because of the toxicity of chemical reducers such as CTAB. Furthermore, the reduction of Ag^+ on the surface of the microbial surface (outer layer surface mode of action) In details, the fungal *Aspergillus niger* (RCMB 002 F008) was inoculated in fungal culture (MGYP broth media). Then, 500 ppm of $AgNO_3$ dissolved in the fungal culture and adjusted the pH with a value of 6.2. The growth of culture was completed in aerobic conditions at temperature of 28°C at 200 rpm in shaker incubator for duration of 5 days. Sterile deionized distilled water was used to complete the sterile filtration and re-suspension processes.

Characterization of silver nanoparticle

Characterization of nanoparticles has been completed through utilization of several physiochemical techniques like X-Ray diffraction analysis. The morphology was examined by two methods which include transmission electron microscopy and scanning electron microscopy. Malvern Zetasizern 3000 HSA was utilized to obtain information about polydispersity index, Particle size and zeta potential. A dilution to appropriate concentraion which is 10-fold using DMEM medium has been achieved and samples were examined immediately. Experiments have been conducted as triplicate.

Obtaining of cell lines

The American Type Culture Collection was used as source to obtain MCF-7 cells. Maintenance of cells was achieved in conditions include 95% air, 5% CO_2 and temperature of 37°C. DMEM medium was fortified by 10% FBS and 1% PS for the sake of doing subculturing and experiments.

Estimation of cell viability

The measurement of how much the MCF-7 cell line was viable has been examined using MTT assay [14]. To sum up the process, A 96-well plates were seeded by 1 × 10^5 cells/well then treatment with silver nanoparticles at several concentrations which involved 100 µg/ ml , 50 µg/ ml, 25 µg/ ml, 12.5 µg/ ml and 6.25 µg/ ml as a negative control for a total of 24 hours. Furthermore, culture medium has been discharged from each individual well to prevent interference of silver nanoparticles, and then a new fresh medium has been putted instead of it, including MTT solution with a concentraion of 0.5 mg/ml, the amount added to be matching to 10% of the culture volume and the incubation has taken a duration of 4 hours with a temperature of 37°C till the formazan product that is characterized by its purple color developed. Acidified isopropanol was used to dissolve the formazan product. Furthermore, an amount equals to 100 ml of the supernatant has been placed in the other fresh wells, and at wavelength equals to 570 nm, the absorbance was obtained using a microplate reader.

Nuclear DNA content estimation

At 70-80% con-fluence, silver nanoparticles at variety of concentrations have been used to treat MCF-7 cells (1 × 10^6) which were placed in T520 flasks. After completion of 24 h, cells harvesting has been done using 0.25% trypsin. At −20°C and for 30 minutes, fixation of cells was achieved using 70% ice cold ethanol. Collection of pellets was done then washing was accomplished using PBS. Re-suspension was done in amount of 500 µl PBS with 20 µl RNAse (5 mg/ml) in it and for 30 min at 37°C, staining using PI (1 mg/ml) was completed. The estimation of cells has been achieved by flow cytometry.

Apoptosis assay

After seeding the cells in T520 flasks and execution of the same steps those have been followed in the DNA content estimation except for using Annexin V-FITC/PI staining protocol for apoptosis detection instead of PI alone, MCF-7 cells viability has been measured through utilization of flow cytometry.

Oxidative stress and Antioxidant biomarkers

Breast cancer MCF-7 was obtained from ATCC, USA. In brief, 1 x 10^4 cells/well were seeded in 96-well plates and exposed for 24 hours to 50 µg/ml of silver nanoparticles. Whole cell lysate was prepared after 24 hours of cell culture for oxidative and anti-oxidative assays. Through using the same methodology described by Ohkawa et al. (1979), cells have been examined for lipid peroxidation through measurement of thiobarbituric acid reactive substances as a marker [12]. Furthermore, level of nitrate/nitrite has been estimated using the same approach that mentioned by Green et al. (1982) [12].

RNA isolation and qRT-PCR

The MCF-7 cells were cultured in six-well plates and exposed to silver nanoparticles (50 mg/ml) for duration of time equals to 24 hours. After that, total amount RNA has been extracted by RNeasy mini Kit. In addition to that, using a Nanodrop 8000 spectrophotometer, the value of concentration of RNA after extraction was obtained. QuantiTect SYBR Green PCR Kit was used to evaluate the mRNA expression of the genes that were identified (Qiagen, USA). For normalization, Ct values for the housekeeping gene GAPDH were used. To estimate fold changes in the expression of the identified genes, the following PCR conditions were used: 94°C for 5 min, 40 cycles (94°C for 30 sec, 60°C for 30 sec, and 72°C for 45 sec). To estimate the relative gene expression suggested by fold variations in measured mRNA, delta-delta Ct equations have been applied.

Table 1: the list the primers used in the RT-PCR assay

Primer	Sequence (5'-3')
LC3	F: TGCAGATTATGCGGATCAAACC
	R: GCATTCACATTTGTTGTGCTGTAG
mTOR	F: AGAAGGGTCTCCAAGGACGACT
	R: GCAGGACACAAAGGCAGCATTG
AKT	F: TTCTGCAGCTATGCGCAATGTG
	R: TGGCCAGCATACCATAGTGAGGTT
GAPDH	F: GTCTCCTCTGACTTCAACAGCG
	R: ACCACCCTGTTGCTGTAGCCAA

Immunohistochemical examination

Immunohistochemical staining has been applied to paraffin-embedded sections after completion of the deparaffinization process in the sake of detection of Caspase-3 enzyme and AKT antibody. Using sodium citrate buffer that has a concentration of 10 mM, the sections have been microwaved for 20 minutes. Incubation for 20 minutes in hydrogen peroxide which has a concentration of 3.0% has been done to stop endogenous peroxidase activity. An overnight incubation at temperature of 4°C in AKT at 1:200 dilution and primary caspase-3 at 1:100 dilution has been done after washing with PBS. Moreover, additional incubation with biotinylated secondary antibody for duration of time equals to 30 minutes was done to the sections after getting washed by PBS. Furthermore, Images have been exposed to analysis using Image Pro Plus software after being incubated with streptavidin–biotin–peroxidase complex, a solution 3–30 diaminobenzidine containing 1.0 % hydrogen peroxide, and lightly counterstained with Harris hematoxylin.

Transmission electron microscope (TEM)

MCF-7 cells have been treated by silver nanoparticles at concentration of 50 µg/ml for several durations of time equal to 3, 6, 12 and 24 hours. After the end of nanoparticles treatment, cells have been gathered, washed by using PBS and the ice-cold glutaraldehyde (2.5%) was used to fixate the cells for 1 hour. Furthermore, the cells have been washed using PBS 3 times for 15 min then fixed in OsO_4 (1%) for 1 hour. Staining using uranyl acetate (2%) has been done at room temperature for 30 min. Dehydration of cells has been achieved using serial dilutions of ethanol (50, 70, and 90%) for 15 minutes each. Further steps were involved placing the cells for 20 minutes in 100% ethanol and another 20 minutes in 100% acetone. Moreover, the cells have been immersed in Epon812 and ultrathin sections (120 nm) were gained and stained

through using both of uranyl acetate (2%) for 20 min and lead citrate for 5 min. The sections were examined using Field Emission Transmission Electron Microscopy has been done after that and the results obtained.

Quantitative analysis

Quantitative analysis results have been expressed in the form of mean ± standard deviation of experiments that have been done in triplicate. The Student's t test was used to compare the means between two samples. Analysis was done using SPSS 17.0 software.

RESULTS

Characterization of silver nanoparticle

The physicochemical features of the synthesized silver nanoparticles have been studied through using XRD, TEM and SEM techniques. As figure 1 shows, the results of XRD for Biosynthesized silver nanoparticles revealed major diffraction peaks at 2 Θ = 35.634, 43.415 and 65.264°, which are related to 111, 220, and 400, respectively. As figure 2 displayed, the hydrodynamic size and zeta potential were measured at 24 h in serum-free DMEM as the following: the hydrodynamic size was 75 nm with the zeta potential equal - 30 mV with PDI 0.10. These data indicated that the prepared Ag-NPs possessed favorable stability and monodispersity in both stock solution and culture medium. As figure 3 shows, the SEM results display the surface morphology features of silver nanoparticles which indicate that the nanoparticles are having spherical shapes with smooth surface. Additionally, TEM images demonstrate the size of silver nanoparticle which is ranged from 14 to 16 nm, as revealed in figure 4.

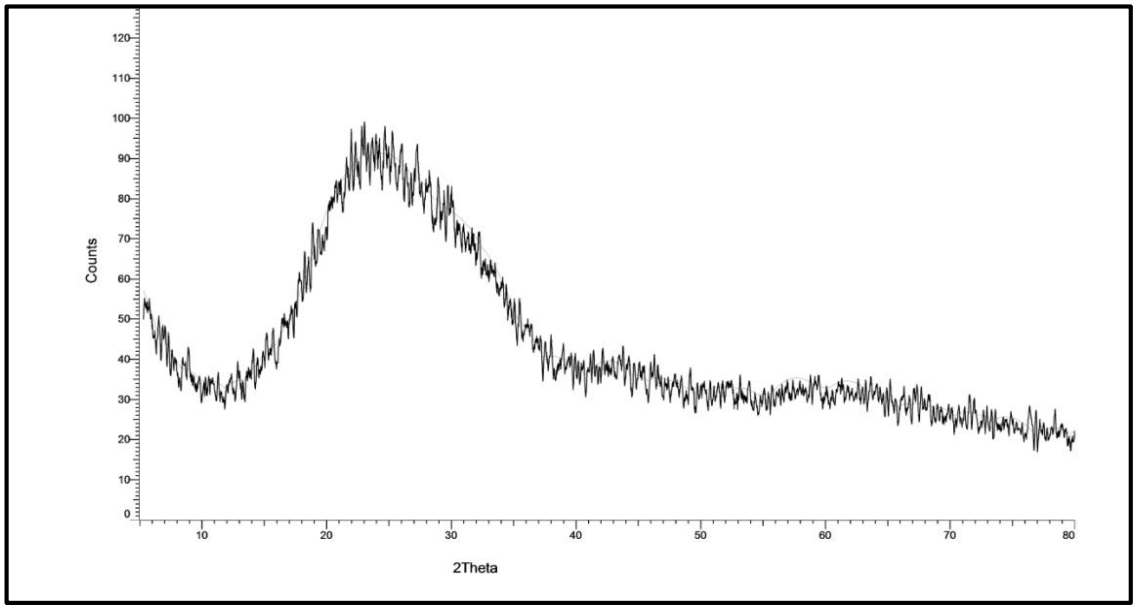

Figure 1: XRD of silver nanoparticles synthesized using green methods

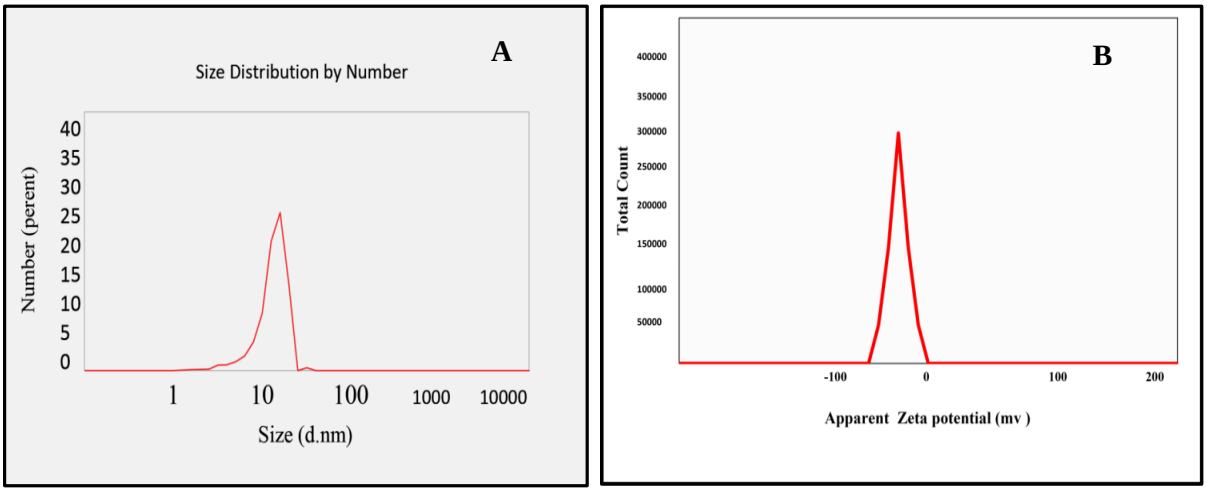

Figure 2: The hydrodynamic size and zeta potential of AgNPs synthesized using green methods in DMEM at 24 h. (A). DLS (nm) (B). Zeta potential (mV).

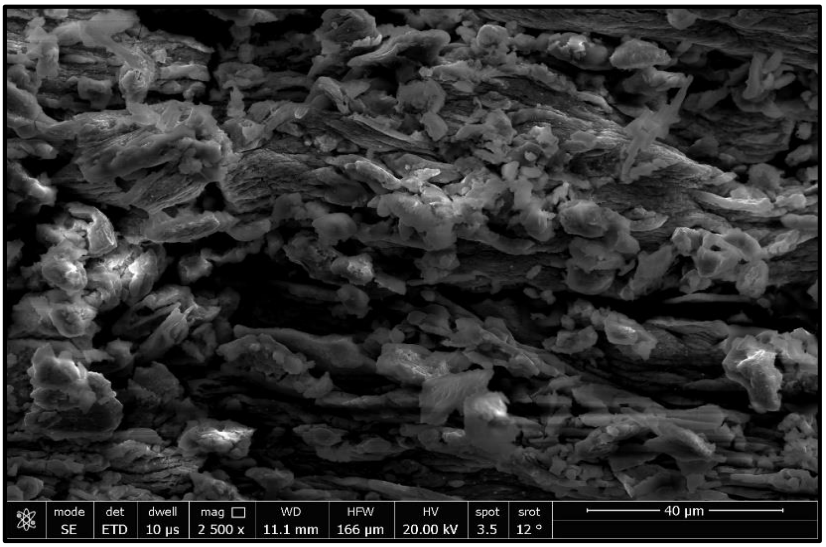

Figure 3: SEM image of silver nanoparticles synthesized using green methods

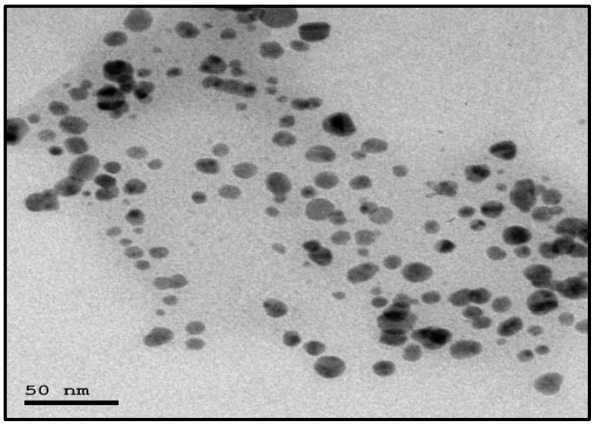

Figure 4: TEM image of silver nanoparticles synthesized using green methods

Estimation of cell viability

Using MTT technique and as it has been shown in figure 5, the viability of breast cancer MCF 7 cells was decreased from 100% at 0.5 µg/ml to less than 20% Ag-NPs after being treated with 100 µg/ml of Ag-NPs for 24 hour.

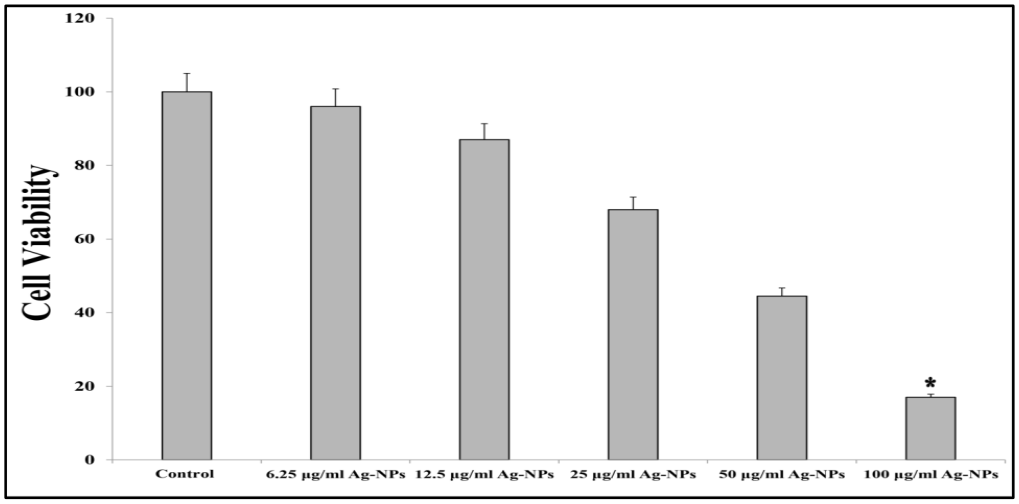

Figure 5: cell viability of MCF 7 cell after treatment with different concentrations silver nanoparticles synthesized using green methods for 24 hours.

DNA content estimation

After 24 h treatment MCF7 with silver nanoparticles, the cell cycle phase was evaluated by using flow cytometry with propidium iodide (PI) staining. As shown in figure 6, Ag-NPs Treatment enhanced the accumulation of the MCF 7 cells at the S phase significantly ($P<0.05$) compared with the control. The percentages of the cells at S increase significantly ($P<0.05$) with increasing silver nanoparticles concentration. The growth of the MCF 7 treated with 50 µg/ml silver nanoparticles was about 55.61, 12.93 and 31.46 % at G0/1, G2/M, and S, respectively, in comparison with negative control cells, in which the growth estimated to be about 50.08, 7.61, and 42.31 % at G0/1, G2/M, and S, respectively, which declared that the cell cycle arrest at S phase.

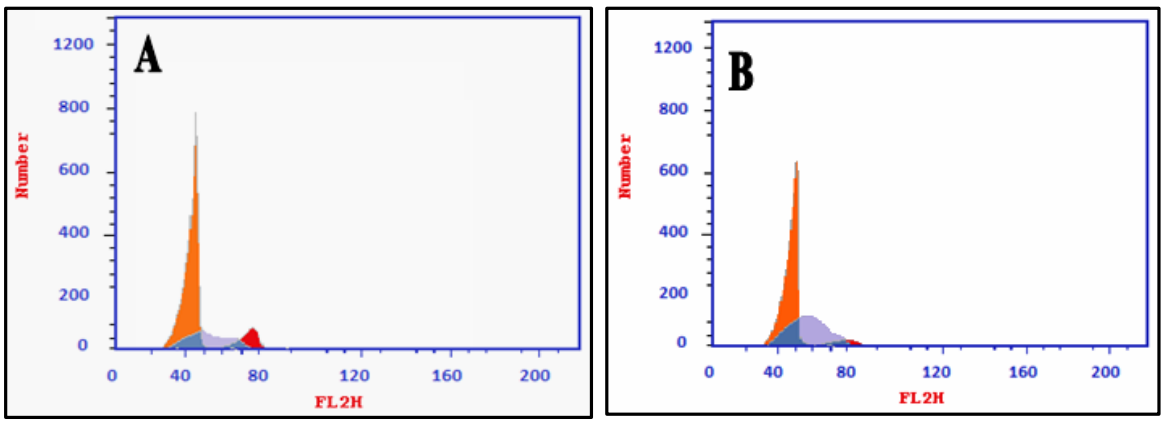

Figure 6: DNA content estimation of MCF-7 cell line after treatment with of Silver nanoparticles.

a) Non-treated cell line
b) Cell line treated with 50 µg/ml of silver nanoparticles

MCF-7 cells are induced to apoptosis by silver nanoparticles

As shown in figures 7 (A and B), The flow cytometric analysis results of silver nanoparticles induced apoptosis in MCF-7 cells using Annexin V-FITC/PI staining showed that the relationship between percentage of apoptotic cells and concentration of silver nanoparticles is directly proportional.

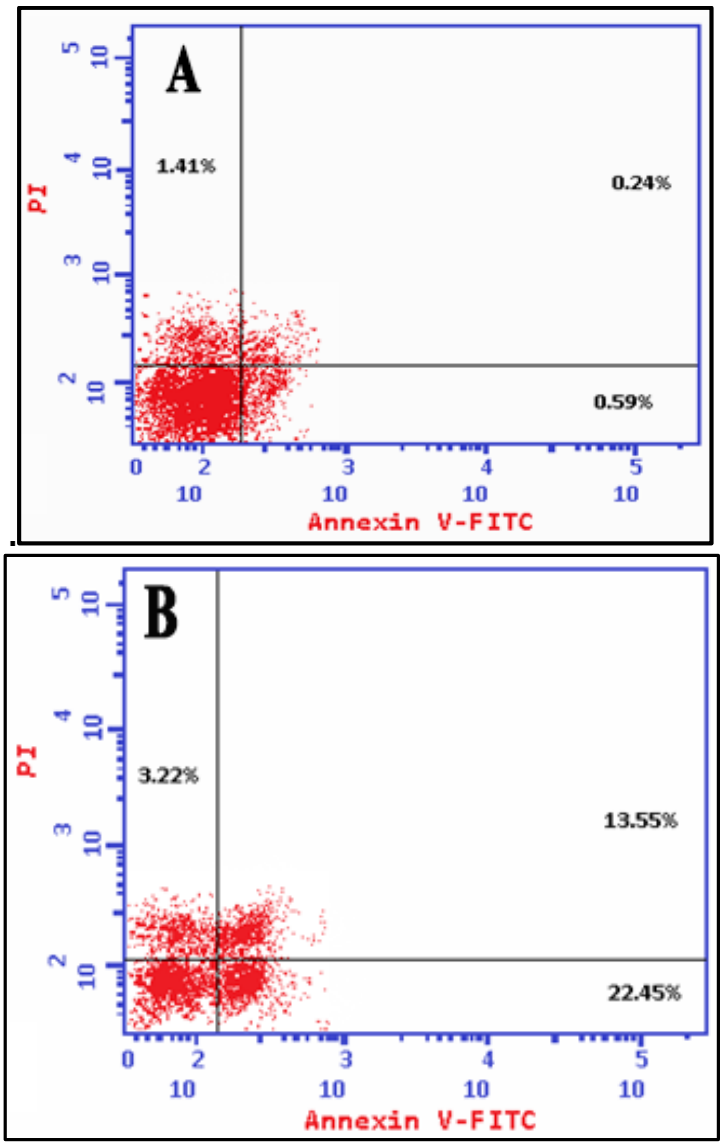

Figure 7: results of apoptosis assay after applying Annexin V-FITC/PI stain on the cells.

a) Non-treated cell line

b) Cell line treated with 50 µg/ml of silver nanoparticles

Quantitative RT-PCR

The levels of apoptotic genes (LC3, AKT, and m-TOR) in the MCF-7 cell have been examined by silver nanoparticles treatment at a concentration of 50 µg/ml for a total of 24 h. The results are showing alteration in genes expression in MCF-7 cells. The mRNA expression levels of the autophagic genes LC3 (Figure 8A), AKT (Figures 8B), and mTOR were significantly unregulated.

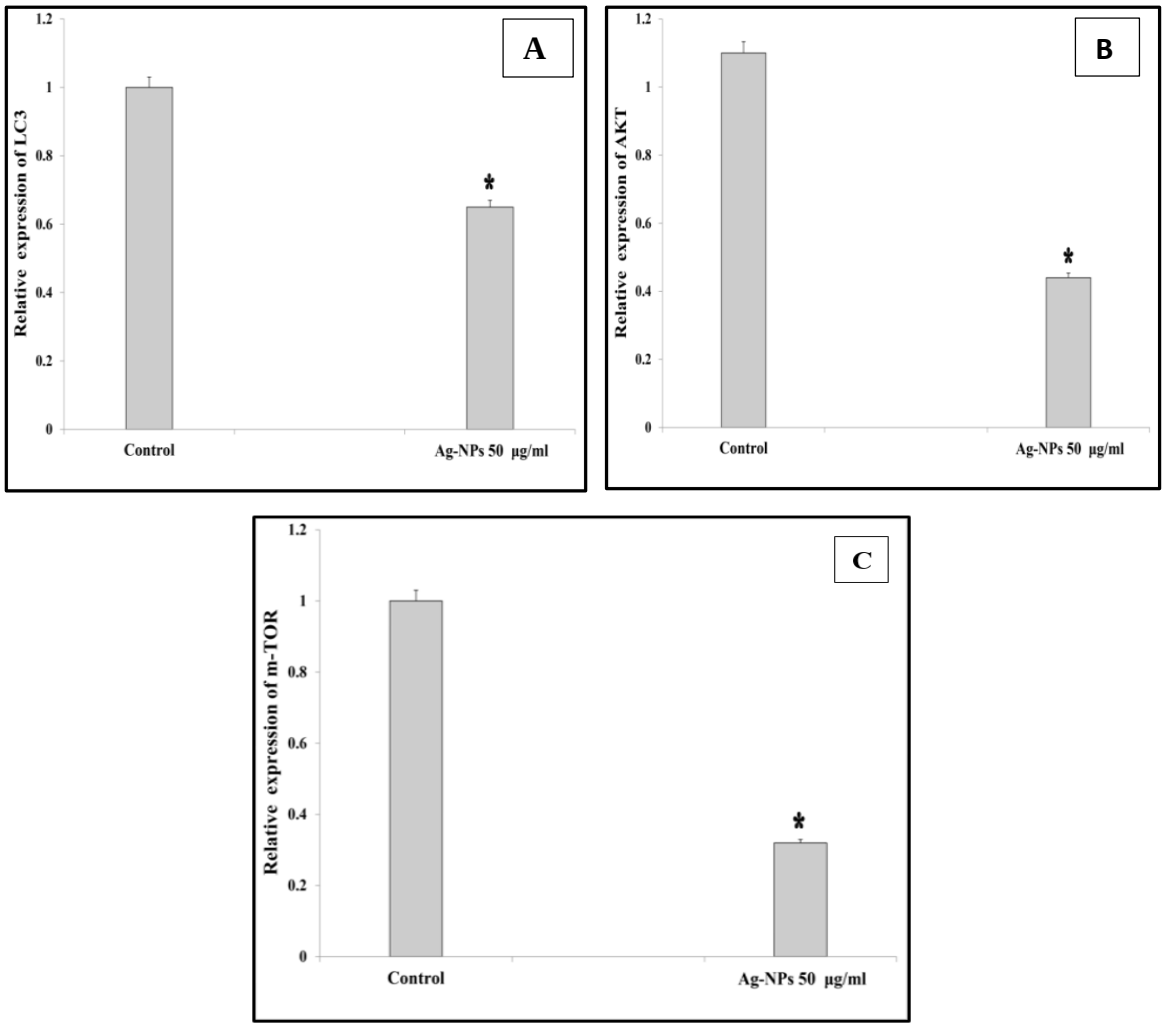

Figure 8: Results of quantitative real-time PCR measure which are showing mRNA levels after 50 µg/ml of Ag-NPs treatment for duration of 24 hour.*Statistically significant difference in comparison with the control (P >0.05 for each). (A) LC3 (B) AKT (C) mTOR.

Oxidative stress and antioxidant biomarkers

The MDA assay is considered as lipid peroxidation biomarker, which refers to oxidative stress. Figure 9 a show a significant increase in oxidative stress mediators. MDA concentrations were reduced two-fold when compared to the negative control. The concentration of MDA was increases from 3.7 nmol/ml at a concentration of 50 µg/ml silver nanoparticles, as compared with the negative control. Also, silver nanoparticles increase the concentration of nitric oxide as antioxidant marker with three-fold as compared with negative control. The concentration of NO was increases to 43 µmol/ml at a concentration of 50 µg/ml silver nanoparticles.

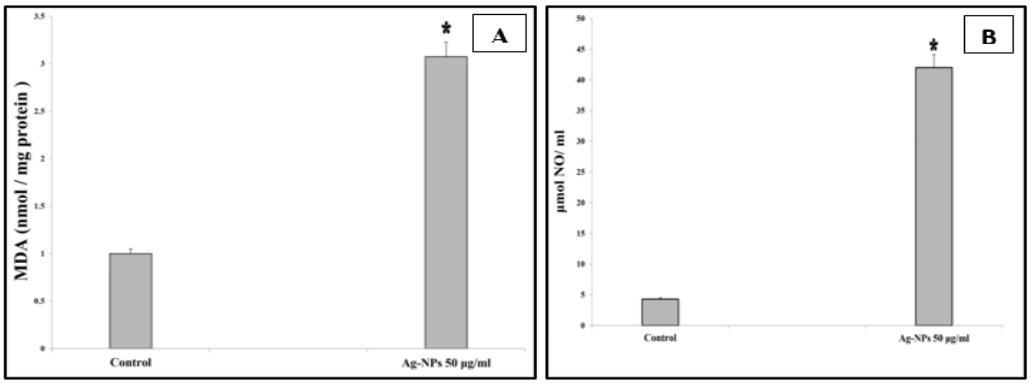

Figure 9: Oxidative and ant oxidative stress markers of breast cancer cell MCF 7 cells after treated with 50 µg/mL Ag-NPs. *Statistically significant difference in comparison with the control (P > 0.05 for each). (A) MDA (B) NO.

Immunohistochemical examination

Weaker AKT was immunohistochemically observed in MCF-7 as silver nanoparticles interacted with it, as shown in Figure 10 b, as compared with the negative control (Figure 10 a). While Caspase 3 has a strong immunohistochemical presence in MCF-7, as shown in Figure 11B, as compared with the negative control

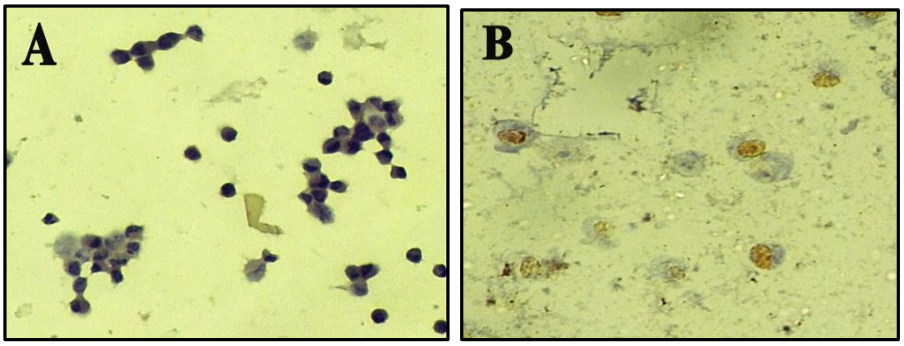

Figure 10: The effect of AKT expression immunoreactivity by silver nanoparticles on MCF 7 cell line according to immunohistochemistry

a) Non-treated cell line
b) Cell line treated with 50 µg/ml of silver nanoparticles

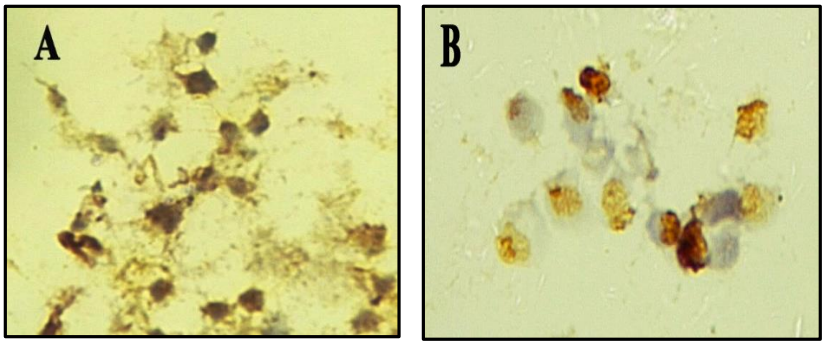

Figure 11: The effect of Caspase 3 expression immunoreactivity by silver nanoparticles on MCF 7 cell line according to immunohistochemistry

a) Non-treated cell line
b) Cell line treated with 50 µg/ml of silver nanoparticles

Transmission electron microscope (TEM)

TEM technique displays the distinctive features of autophagosome accumulation associated with apoptotic cell stages: In the non-treated cell, there is an observed cell with a normal subcellular organelle morphology with a few autophagic vacuoles (Figure.12A).While a number of autophagosomes and single-membrane autolysosomes were present as Ag-NPs treated at a concentration of 50 µg/ml after 6 hours, as Figure 12B showed.

Furthermore, autophagosomes engulfed particle aggregates, damaged mitochondria and misfolded proteins, as being displayed in Figure 12 B. Morphologically, the cells rounded up with vanishing of cytoplasmic. Secondly, there were several changes happened as the time increased from 12 hours to 24 hours because of chromatin condensation at the nuclear periphery mitochondria, which is carried out during treatment as shown in figures 12 C and D.

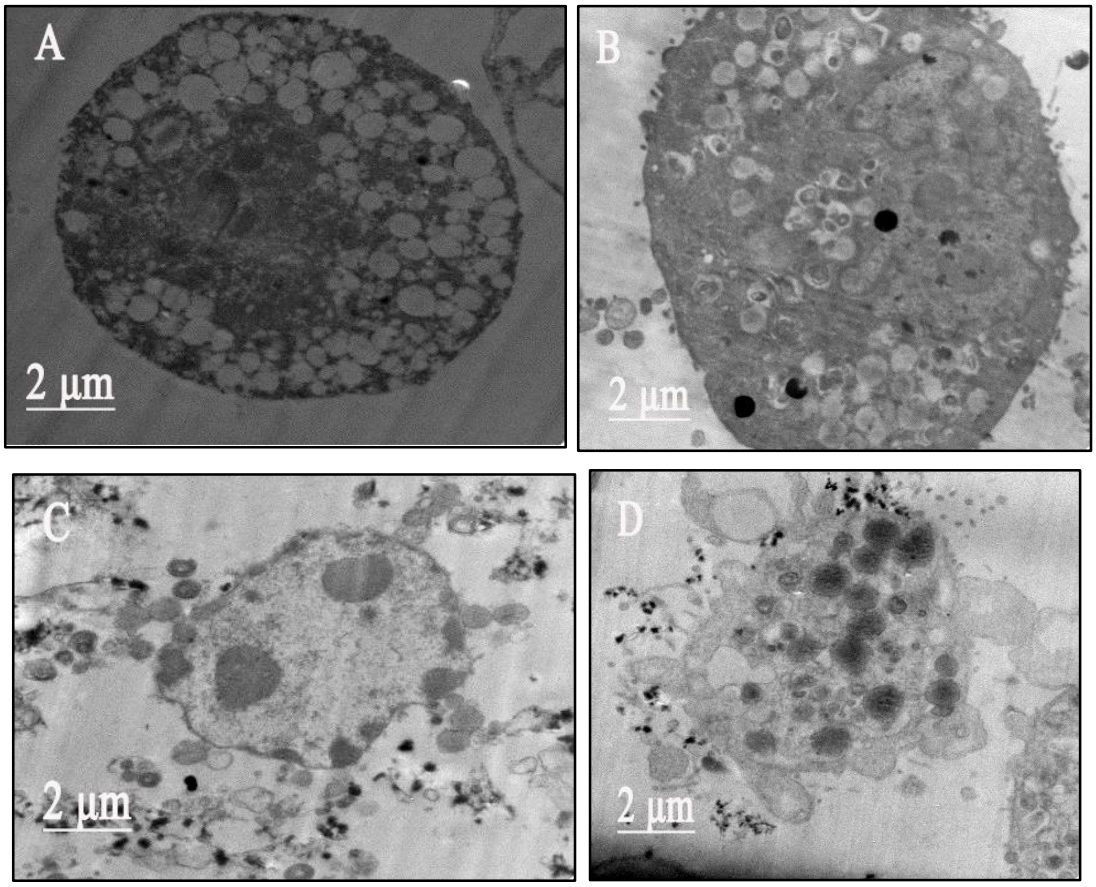

Figure 13: results obtained using transmission electron microscope on MCF-7 cells treated with a silver nanoparticles concentration that equals to 50 µg/ml for different durations. (A) Control cell. (B) Treatment for 6 hour. (C) Treatment for 12 hour. (D) Treatment for 24 hour.

DISCUSSION

Currently, breast cancer is classified as an aggressive cancer, leading to cancer mortality among women around the world [23]. It was carried out at two sites in the breast lobular and in the ducts [2]. Silver nanoparticles have attracted the interest of modern science due to their brilliant applications, especially in medical science [24–

25]. Silver nanoparticles are used in many biological fields, such as antibacterial, antifungal, anti-inflammatory, antiviral, and anticancer [26–27]. Also, the silver nanoparticle successfully inhibits the HIV virus from binding to the host cell *in vitro* [28]. There are many methods to prepare silver nanoparticles; for example, a biological approach using microbial fermentation is more facile, clean, nontoxic, cost-effective, and environmentally friendly [29]. Silver nanoparticles are approved by the US Food and Drug Administration (FDA) for use as antibacterial wound dressings, food supplements, and medical devices. The utilization of Ag-NPs as anticancer agents is due to their ability to generate reactive oxygen species (ROS), leading to ATP synthesis arrest and DNA damage [30–31].

Previous work demonstrated silver nanoparticles against breast (SKBR3 and 8701-BC), leukemia, and colon (HT-29, HCT116, and Caco-2) cancer cells [32–35]. Macroautophagy is a response to regulation that degrades cellular organelles and macromolecules [36]. There are many factors controlling the process of the autophagy pathway; one of these factors is mTORC1, which controls autophagy indirectly by negatively regulating the transcription of genes required for lysosome biogenesis [36]. In this work, silver nanoparticles were synthesized by reduction of silver nitrate by Aspergillus *niger and* then characterized by physiochemical techniques such as XRD, DLS, Zeta potential, SEM, and TEM.

Consequently, we investigated the toxicity of Ag-NPs using the MTT assay, the apoptosis and cell cycle arrest, and the ability of silver nanoparticles to induce apoptosis and autophagy by RT-PCR, immunohistochemistry, and TEM analysis. The results showed that the preparation of silver nanoparticles in a regular shape with particle sizes of 14–16 nm and a zeta potential equal to 30 mV with PDI 0.10 The cell cycle arrest of MCF7 after treatment with 50 µg/ml silver nanoparticles was about 55.61, 31.46, and 12.93% at G0/1, G2/M, and S, respectively. This indicated that the cell cycle was in S phase. Furthermore, the percentage of apoptotic cells increased with the increasing concentration of silver nanoparticles, from 2.24 to 39.22%, respectively. The mRNA expression of the following genes, LC3, AKT, and mTOR, was significantly unregulated. Also, the immunohistochemical assay showed a weaker AKT as silver nanoparticles interact with breast cancer cell MCF-7, while caspase 3 is observed. TEM analysis of breast cancer cell MCF-7 after remediation with silver nanoparticles at different times demonstrated the typical features of autophagosome accumulation associated with apoptotic cell stages. Furthermore, autophagosomes engulfed particle aggregates, damaged mitochondria, and misfolded proteins, as shown in figures 12 b, c, and d. Finally, these results indicate that the cytotoxicity of Ag-NPs may involve the autophagic pathway in MCF-7 cells.

CONCLUSION

In this work, silver nanoparticles are synthesized by *Aspergillus niger* as a reducing agent under aerobic conditions at pH 6.2 (weak acid medium). Consequently, silver nanoparticles were characterized using physiochemical techniques such as XRD, DLS, SEM, and TEM. The physicochemical data confirmed the formation of silver nanoparticles with diameters of 14–16 nm. Also, in this work, the silver nanoparticles investigated the autophagy mechanism against breast cancer cell MCF-7 through different tools such as apoptosis, DNA content, oxidative and ant-oxidative stress markers, RT-PCR, immunohistochemistry, and transmission electron microscopy. The results revealed that silver nanoparticles activated apoptosis at 39.2% and arrested

the cell cycle at S phase due to an increase in the percentage of cells at S of 10 percent as compared with the negative control. Furthermore, the rt-Pcr results showed downregulation of LC3, AKT and mTOR. The LC3 gene is an autophagic gene that regulates the autophagy process. The immunohistochemistry showed weaker AKT, while Caspase 3 showed strong immunochemistry staining. Transmission electron microscopy showed autophagosomes that are considered the benchmark for autophagy studies; the number of double-membrane autophagosomes and single-membrane autolysosomes was obviously observed in Ag-NP-treated MCF-7. Finally, these results indicate that the cytotoxicity of Ag-NPs may involve the autophagic pathway in MCF-7 cells.

Data Availability

Contributions which found in the study are existed in the article; additional questions can be directed to the corresponding author.

Acknowledgment

The researchers would like to acknowledge Deanship of Scientific Research, Taif University for funding this

work.

Conflicts of Interest presence

In regard to author's declaration, the research has been conducted without any conflict of interest.

Author contributions

Conceptualization: Fawziah A. Al-Salmi; formal analysis: Fawziah A. Al-Salmi funding acquisition: Fawziah A. Al-Salmi, : investigation: Fawziah A. Al-Salmi; investigation, Fawziah A. Al-Salmi project administration: Fawziah A. Al-Salmi; Resource: Fawziah A. Al-Salmi, ; supervision: Fawziah A. Al-Salmi; Validation: Fawziah A. Al-Salmi visualization: Fawziah A. Al- Salmi ; writing original draft: Fawziah A. Al-Salmi: writing -review edition; Fawziah A. Al-Salmi. The author approved the final version of the manuscript.

References

1) Akram M, Iqbal M, Daniyal M, Khan AU. Awareness and Current Knowledge of Breast Cancer. Biol Res (2017) 50:33. doi: 10.1186/s40659-017-0140-9

2) Sharma GN, Dave R, Sanadya J, Sharma P, Sharma KK. Various Types and Management of Breast Cancer: An Overview. J Adv Pharm Technol Res (2010) 1:109–26. doi: 10.4103/2231-4040.79794

3) Zafrakas M, Papasozomenou P, Emmanouilides C. Sorafenib in Breast Cancer Treatment: A Systematic Review and Overview of Clinical Trials. World J Clin Oncol (2016) 7:331–6. doi: 10.5306/wjco.v7.i4.331.

4) Qu Y, Kang M, Cheng X and Zhao J (2020) Chitosan-Coated Titanium Dioxide-Embedded Paclitaxel Nanoparticles Enhance Anti-Tumor Efficacy against Osteosarcoma. Front. Oncol. 10:577280. doi: 10.3389/fonc.2020.577280.

5) L. Zhang, X. M. Ji, X. X. Yang, and X. Zhang, "Cell type- and density-dependent effect of 1 T static magnetic field on cell proliferation," Oncotarget, vol. 8, no. 8, pp. 13126–13141,2017.

6) Zapevalova, M.V.; Shchegravina, E.S.; Fonareva, I.P.; Salnikova, D.I.; Sorokin, D.V.; Scherbakov, A.M.; Maleev, A.A.; Ignatov, S.K.; Grishin, I.D.; Kuimov, A.N.; et al. Synthesis, Molecular Docking, In Vitro and In Vivo Studies of Novel Dimorpholinoquinazoline- Based Potential Inhibitors of PI3K/ Akt/mTOR Pathway. Int. J. Mol. Sci. 2022, 23, 10854. https://doi.org/10.3390/ijms231810854

7) Jiang, N.; Dai, Q.; Su, X.; Fu, J.; Feng, X.; Peng, J. Role of PI3K/AKT Pathway in Cancer: The Framework of Malignant Behavior. Mol. Biol. Rep. 2020, 47, 4587–4629. [CrossRef]

8) Revathidevi, S.; Munirajan, A.K. Akt in Cancer: Mediator and More. Semin. Cancer Biol. 2019, 59, 80–91. [CrossRef]

9) Yang, H.; Rudge, D.G.; Koos, J.D.; Vaidialingam, B.; Yang, H.J.; Pavletich, N.P. MTOR Kinase Structure, Mechanism and Regulation.Nature 2013, 497, 217–223. [CrossRef]

10) Zou, Z.; Tao, T.; Li, H.; Zhu, X. MTOR Signaling Pathway and MTOR Inhibitors in Cancer: Progress and Challenges. Cell Biosci. 2020, 10, 31.

11) O. Yesil-Celiktas, C. Sevimli, E. Bedir, F. Vardar-Sukan, Inhibitory effects of rosemary extracts, carnosic acid and rosmarinic acid on the growth of various human cancer cell lines, Plant Foods Hum. Nutr. 65 (2010) 158–163, https://doi.org/10. 1007/s11130-010-0166-4.

12) J.S. Liu, C.Y. Huo, H.H. Cao, C.L. Fan, J.Y. Hu, L.J. Deng, Z.B. Lu, H.Y. Yang, M.Z.X. Yu LZ, Z.L. Yu, Aloperine induces apoptosis and G2/M cell cycle arrest in hepatocellular carcinoma cells through the PI3K/Akt signaling pathway, Phytomedicine 61 (2019) 152843, , https://doi.org/10.1016/j.phymed.2019. 152843

13) Y. Liu, X.B. Zhang, J.J. Liu, S. Zhang, J. Zhang, NVP-BKM120 in combination with letrozole inhibit human breast cancer stem cells via PI3K/mTOR pathway, Zhonghua Yi Xue Za Zhi 99 (2019) 1075–1080, https://doi.org/10.3760/cma.j.issn. 0376-2491.2019.14.008.

14) S. Noorolyai, N. Shajari, E. Baghbani, S. Sadreddini, B. Baradaran, The relation between PI3K/AKT signalling pathway and cancer, Gene 698 (2019) 120–128, https://doi.org/10.1016/j.gene.2019.02.076.

15) Wu N, Zhu Y, Xu X, et al. The anti-tumor effects of dual PI3K/mTOR inhibitor BEZ235 and histone deacetylase inhibitor Trichostatin A on inducing autophagy in esophageal squamous cell carcinoma. J Cancer 2018; 9: 987–997. 7.

16) Ito K, Caramori G and Adcock IM. Therapeutic potential of phosphatidylinositol 3-kinase inhibitors in inflammatory respiratory disease. J Pharmacol Exp Ther 2007; 321: 1–8. 8.

17) Zhang X, Kong Y, Sun Y, et al. Bone marrow mesenchymal stem cells conditioned medium protects VSC4.1 cells against 2,5-hexanedione-induced autophagy via NGF-PI3K/Akt/mTOR signaling pathway. Brain Res 2018; 1696: 1–9.

18) Hassan A, Elebeedy D, Matar ER, Fahmy Mohamed Elsayed A and Abd El Maksoud AI (2021) Investigation of Angiogenesis and Wound Healing Potential Mechanisms of Zinc Oxide Nanorods. Front. Pharmacol. 12:661217. doi: 10.3389/fphar.2021.661217.

19) Hassan, A., AL-Salmi, F. A., Saleh, M. A., Sabatier, J. M., Alatawi, F. A., Alenezi, M. A., ... & Sharaf, E. M. (2023). Inhibition Mechanism of Methicillin-Resistant Staphylococcus aureus by Zinc Oxide Nanorods via Suppresses Penicillin-Binding Protein 2a. ACS Omega.

20) Hassan A, Al-Salmi FA,Abuamara TMM, Matar ER, Amer ME,Fayed EMM, Hablas MGA, Mohammed TS, Ali HE,Abd EL-fattah FM, Abd Elhay WM,Zoair MA, Mohamed AF, Sharaf EM, Dessoky ES, Alharthi F, Althagafi HAEand Abd El Maksoud AI (2022)Ultrastructural analysis of zinc oxidenanospheres enhances anti-tumor efficacy against Hepatoma. Front. Oncol. 12:933750.doi: 10.3389/fonc.2022.933750.

21) Sharaf EM, Hassan A, AL-Salmi FA, Albalwe FM, Albalawi HMR, Darwish DB and Fayad E (2022) Synergistic antibacterial activity of compact silver/magnetite core-shell nanoparticles core shell against Gram-negative foodborne pathogens.Front. Microbiol. 13:929491. doi: 10.3389/fmicb.2022.929491

22) Calderón-Jiménez B, Johnson ME,Montoro Bustos AR, Murphy KE,Winchester MR and Vega Baudrit JR(2017) Silver Nanoparticles:Technological Advances, Societal Impacts, and Metrological Challenges. Front. Chem. 5:6.doi: 10.3389/fchem.2017.00006.

23) Siegel R., Naishadham d. and Jemal A.: Cancer statistics. CA. Cancer. J. Clin., 63 (1): 11-30, 2013.

24) K. Yokohama and D. R. Welchons, “-e conjugation of amyloid beta protein on the gold colloidal nanoparticles surfaces,” Nanotechnology, vol. 18, no. 10, pp. 105101–105107,2007.

25) V. K. Sharma, R. A. Yngard, and Y. Lin, “Silver nanoparticles: green synthesis and their antimicrobial activities,” Advances in Colloid and Interface Science, vol. 145, no. 1-2, pp. 83–96, 2009.

26) K. K. Wong and X. Liu, “Silver nanoparticles—the real “silver bullet” in clinical medicine?,” MedChemComm, vol. 1, no. 2, pp. 125–131, 2010.

27) D. R. Monteiro, S. Silva, M. Negri et al., “Silver nanoparticles: influence of stabilizing agent and diameter on antifungal activity against Candida albicans and Candida glabrata biofilms,” Letters in Applied Microbiology, vol. 54, no. 5, pp. 383–391, 2012.

28) C. Krishnaraj, R. Ramachandran, K. Mohan, and P. T. Kalaichelvan, “Optimization for rapid synthesis of silver nanoparticles and its effect on phytopathogenic fungi,” Spectrochimica Acta Part A: Molecular and Biomolecular Spectroscopy, vol. 93, pp. 95–99, 2012.

29) J. Favero, P. Corbeau, M. Nicolas et al., “Inhibition of humanimmunodeficiency virus infection by the lectinjacalin and by a derived peptideshowing a sequence similarity with gp120,” European Journal of Immunology, vol. 23, no. 1, pp. 179–185, 1993.

30) Medici, S.; Peana, M.; Nurchi, V. M.; Zoroddu, M. A. Medical uses of silver: history, myths, and scientific evidence. J. Med. Chem. 2019, 62, 5923−5943.

31) Bhattacharya, R.; Mukherjee, P. Biological properties of “naked” metal nanoparticles. Adv. Drug Delivery Rev. 2008, 60, 1289−1306.

32) Gomathi, A.; Rajarathinam, S. X.; Sadiq, A. M.; Rajeshkumar, S. Anticancer activity of silver nanoparticles synthesized using aqueous fruit shell extract of Tamarindus indica on MCF-7 human breast cancer cell line. J. Drug. Deliv. Sci. Technol. 2020, 55, 101376.

33) Morais, M.; Teixeira, A. L.; Dias, F.; Machado, V.; Medeiros, R.; Prior, J. A. Cytotoxic Effect of Silver Nanoparticles Synthesized by Green Methods in Cancer. J. Med. Chem. 2020, 63, 14308−14335.

34) Barabadi, H.; Vahidi, H.; Rashedi, M.; Mahjoub, M. A.; Nanda, A.; Saravanan, M. Recent advances in biological mediated cancer research using silver nanoparticles as a promising strategy for hepatic cancer therapeutics: a systematic review. Nanomed. J. 2020, 7, 251− 262.

35) Sukirtha, R.; Priyanka, K. M.; Antony, J. J.; Kamalakkannan, S.; Thangam, R.; Gunasekaran, P.; Krishnan, M.; Achiraman, S. Cytotoxic effect of Green synthesized silver nanoparticles using Melia azedarach against in vitro HeLa cell lines and lymphoma mice model. Process Biochem. 2012, 47, 273−279.

36) Yang, S., Wang, X., Contino, G., Liesa, M., Sahin, E., Ying, H., ... & Kimmelman, A. C. (2011). Pancreatic cancers require autophagy for tumor growth. *Genes & development*, *25*(7), 717-729.